

conserved near residue 30. These findings indicate that the amino acid residues near position 30 are an essential for TNFR2 binding.

3.3. Binding kinetics of TNFR2-selective TNF mutants

To investigate the properties of eight TNFR2-selective TNF mutants in detail, we prepared recombinant protein using the previously described methods [30,31]. TNF mutants expressed as an inclusion body in *E. coli* (BL21λDE3) were denatured and refolded. Then, active TNF mutants were purified by ion-exchange and gel-filtration chromatography. TNF mutant purity was greater than 90% in sodium dodecyl sulfate–polyacrylamide gel electrophoresis, and all mutants were confirmed to form homotrimers in the same manner as the wtTNF by gel-filtration analysis (data not shown). To analyze the binding properties of these TNFR2-selective TNF mutants, we determined their binding dissociation constants (kinetic on- and off-rates) for TNFR1 and TNFR2, respectively, in detail using the surface plasmon resonance technique (Table 2). Our analysis showed that all eight mutant TNFs bound to the TNFR2 with high affinity; in contrast, they bound to the TNFR1 with greatly reduced affinity (typically between 1 and 7% of the wtTNF affinity). The dissociation constants (K_D) of these mutants for TNFR2 were between 2.1 – 3.6×10^{-10} M, and their relative affinities for TNFR2 were between 169 and 291% of that of the wtTNF. Thus, using the competitive panning technique we successfully obtained a large repertoire of TNFR2-selective TNF mutants with different binding parameters (on- and off-rates and dissociation constants).

3.4. Bioactivities of TNFR2-selective TNF mutants

To examine the bioactivity of these TNF mutants via TNFR1, we subsequently performed a cytotoxicity assay using HEP-2 cells (Fig. 4A and B). All TNF mutants (R2-6 ~ R2-13) showed almost no cytotoxicity, and the bioactivity was much lower than that of the wtTNF. Next, we evaluated the TNFR2-mediated activity of TNF mutants using the hTNFR2/mFas-PA, which were previously constructed in our laboratory [26]. The TNFR2-mediated bioactivities of these 8 mutant TNF proteins were at least same or higher than that of the wtTNF (Fig. 4C and D). As a negative control, we determined TNF cytotoxicity in parental TNFR1^{-/-}R2^{-/-} preadipocytes and observed no wtTNF- or mutant TNF-mediated cell death (data not shown). Results of the cytotoxicity assay are summarized in Table 3. R2-7, the most highly TNFR2-selective mutant, exhibited 1.8×10^5 fold higher TNFR2-selectivity than that for the wild-type TNF.

4. Discussion

Recently, it was revealed that the two TNFRs worked together by crosstalk signaling, which suggested that the TNF-mediated signaling in the presence of both TNF receptors actually correlates with their physiological functions [32–34]. To understand the mechanism as well as to analyze the structure–function relationship of the TNFRs, several attempts were made in the past to create TNFR-specific mutant TNFs by conventional site-directed mutagenesis methods (such as Kunkel's method) [35–37]. However, these attempts were not very successful in yielding a desired TNF mutant having high receptor specificity and full bioactivity. For example, the TNFR2-binding affinity of the double mutant D143N-A145R was about 5–10 fold less than the wtTNF [38]. To overcome these problems, we applied phage-display technique and optimized panning method using the BIAcore biosensor (Fig. 1). Using an adequate amount of selective competitive inhibitor (>1 pmol TNFR1-Fc), this one-step competitive panning is ten times more efficient for screening TNFR2-selective TNF mutants, suggesting the competitive panning technology described here is a simple and effective screening method for fine-tuning TNF receptor-selectivity (Fig. 3). As a result of

screening, we obtained successfully obtained TNFR2-selective TNF mutants with full bioactivity via TNFR2 (Table 3). Because of its high TNFR2-selectivity and full bioactivity, the TNF mutant R2-7 would help in elucidating the functional role of TNFR2.

One advantage of our phage-display-based technique is that it can be used to obtain the sequence information of many mutants [39,40]. It was previously shown by site-specific mutagenesis technique that mutations at positions 29, 31 and 32 (L29S, R31E and R32W) remarkably reduced the TNF's affinity for binding to TNFR2 [35,37,38]. For most of the TNFR2-selective TNF mutants, amino acids at positions 29, 31 and 32 were indeed identical (except for the R2-7 mutant which contained a conserved L to V substitution at position 29) to those of the wtTNF (Table 1), which is consistent with the previously reported idea that these three amino acids play critical roles in maintaining the binding between the TNF and TNFR2. The amino acid sequence at positions 145, 146 and 147 of the TNFR2-selective TNF mutants were, however, very different from those of the wtTNF. For example, the amino acid residue at position 145 of the TNF mutants R2-7, R2-12 and R2-13 contained an Asp residue in place of the Ala residue, and all of them showed high TNFR2 selectivity. Structural analysis and mutagenesis studies suggested that the loop containing the residues 145–147 is involved in the receptor binding [41–43]. Since Asp is a comparatively large residue, we speculated that this substitution could lead to a steric hindrance disrupting the interaction between the TNFR1 and TNFR2-selective mutants, which may be why they are less TNFR1-selective. However, why this replacement would increase the selectivity for TNFR2 is unclear at this moment. Currently, we are working on determining the structure of the TNF/TNFR2 complex by X-ray crystallography [44] so that structure–activity relationship studies could be initiated in the near future. Additionally, this structural information, in combination with bioinformatics technology, will be useful for designing TNFR-selective inhibitors (peptide mimics and chemical compounds).

5. Conclusions

In this study, we optimized our phage display-based screening using a unique competitive panning technique, which is ten times more efficient for screening TNFR2-selective TNF mutants compared to the conventional panning method. As a result of screening, we have succeeded in isolating several TNFR2-specific TNF mutants with high TNFR2 affinity and full bioactivity via TNFR2. Further analysis of the relationship between the structure and bioactivity of the TNF mutants would offer highly valuable and useful information regarding the TNF/TNFR biology. In conclusion, our fine-tuned competitive panning system is a simple and effective technology for isolating receptor-selective mutant proteins.

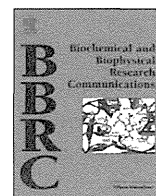
Acknowledgment

This study was supported in part by Grants-in-Aid for Scientific Research from the Ministry of Education, Culture, Sports, Science and Technology of Japan, and from the Japan Society for the Promotion of Science (JSPS). This study was also supported in part by Health Labour Sciences Research Grants from the Ministry of Health, Labor and Welfare of Japan, and by Health Sciences Research Grants for Research on Publicly Essential Drugs and Medical Devices from the Japan Health Sciences Foundation.

References

- Aggarwal BB. Signalling pathways of the TNF superfamily: a double-edged sword. *Nat Rev Immunol* 2003;3(9):745–56.
- Szlosarek PW, Balkwill FR. Tumour necrosis factor alpha: a potential target for the therapy of solid tumours. *Lancet Oncol* 2003;4(9):565–73.

- [3] Aderka D, Engelmann H, Maor Y, Brakebusch C, Wallach D. Stabilization of the bioactivity of tumor necrosis factor by its soluble receptors. *J Exp Med* 1992; 175(2):323–9.
- [4] Feldmann M, Maini RN. Lasker Clinical Medical Research Award. TNF defined as a therapeutic target for rheumatoid arthritis and other autoimmune diseases. *Nat Med* 2003;9(10):1245–50.
- [5] Muto Y, Nouri-Aria KT, Meager A, Alexander GJ, Eddleston AL, Williams R. Enhanced tumour necrosis factor and interleukin-1 in fulminant hepatic failure. *Lancet* 1988;2(8602):72–4.
- [6] Thorbecke GJ, Shah R, Leu CH, Kuruvilla AP, Hardison AM, Palladino MA. Involvement of endogenous tumor necrosis factor alpha and transforming growth factor beta during induction of collagen type II arthritis in mice. *Proc Natl Acad Sci U S A* 1992;89(16):7375–9.
- [7] Williams RO, Feldmann M, Maini RN. Anti-tumor necrosis factor ameliorates joint disease in murine collagen-induced arthritis. *Proc Natl Acad Sci U S A* 1992;89(20):9784–8.
- [8] Gomez-Reino JJ, Carmona L, Valverde VR, Mola EM, Montero MD. Treatment of rheumatoid arthritis with tumor necrosis factor inhibitors may predispose to significant increase in tuberculosis risk: a multicenter active-surveillance report. *Arthritis Rheum* 2003;48(8):2122–7.
- [9] Lubel JS, Testro AG, Angus PW. Hepatitis B virus reactivation following immunosuppressive therapy: guidelines for prevention and management. *Intern Med J* 2007;37(10):705–12.
- [10] Leist M, Gantner F, Jülg S, Wendel A. Activation of the 55 kDa TNF receptor is necessary and sufficient for TNF-induced liver failure, hepatocyte apoptosis, and nitrite release. *J Immunol* 1995;154(3):1307–16.
- [11] Mori L, Iselin S, De Libero G, Lesslauer W. Attenuation of collagen-induced arthritis in 55-kDa TNF receptor type 1 (TNFR1)-IgG1-treated and TNFR1-deficient mice. *J Immunol* 1996;157(7):3178–82.
- [12] Ware CF, Crowe PD, Vanarsdale TL, Andrews JL, Grayson MH, Jerzy R, et al. Tumor necrosis factor (TNF) receptor expression in T lymphocytes. Differential regulation of the type I TNF receptor during activation of resting and effector T cells. *J Immunol* 1991;147(12):4229–38.
- [13] Irwin MW, Mak S, Mann DL, Qu R, Penninger JM, Yan A, et al. Tissue expression and immunolocalization of tumor necrosis factor-alpha in post-infarction dysfunctional myocardium. *Circulation* 1999;99(11):1492–8.
- [14] Dopp JM, Sarafian TA, Spinella FM, Kahn MA, Shau H, de Vellis J. Expression of the p75 TNF receptor is linked to TNF-induced NFkappaB translocation and oxyradical neutralization in glial cells. *Neurochem Res* 2002;27(11):1535–42.
- [15] Yang L, Lindholm K, Konishi Y, Li R, Shen Y. Target depletion of distinct tumor necrosis factor receptor subtypes reveals hippocampal neuron death and survival through different signal transduction pathways. *J Neurosci* 2002; 22(8):3025–32.
- [16] Ban L, Zhang J, Wang L, Kuhlreiber W, Burger D, Faustman DL. Selective death of autoreactive T cells in human diabetes by TNF or TNF receptor 2 agonism. *Proc Natl Acad Sci U S A* 2008;105(36):13644–9.
- [17] Monden Y, Kubota T, Inoue T, Tsutsumi T, Kawano S, Ide T, et al. Tumor necrosis factor-alpha is toxic via receptor 1 and protective via receptor 2 in a murine model of myocardial infarction. *Am J Physiol Heart Circ Physiol* 2007;293(1):H743–53.
- [18] Wang M, Crisostomo PR, Markel TA, Wang Y, Meldrum DR. Mechanisms of sex differences in TNFR2-mediated cardioprotection. *Circulation* 2008;118(Suppl. 14):S38–45.
- [19] Arnett HA, Mason J, Marino M, Suzuki K, Matsushima GK, Ting JP. TNF alpha promotes proliferation of oligodendrocyte progenitors and remyelination. *Nat Neurosci* 2001;4(11):1116–22.
- [20] Faustman D, Davis M. TNF receptor 2 p.thway: drug target for autoimmune diseases. *Nat Rev Drug Discov* 2010;9(6):482–93.
- [21] Fontaine V, Mohand-Said S, Hanoteau N, Fuchs C, Pfizenmaier K, Eisel U. Neurodegenerative and neuroprotective effects of tumor Necrosis factor (TNF) in retinal ischemia: opposite roles of TNF receptor 1 and TNF receptor 2. *J Neurosci* 2002;22(7):RC216.
- [22] MacEwan DJ. TNF receptor subtype signalling: differences and cellular consequences. *Cell Signal* 2002;14(6):477–92.
- [23] Mukai Y, Shibata H, Nakamura T, Yoshioka Y, Abe Y, Nomura T, et al. Structure-function relationship of tumor necrosis factor (TNF) and its receptor interaction based on 3D structural analysis of a fully active TNFR1-selective TNF mutant. *J Mol Biol* 2009;385(4):1221–9.
- [24] Shibata H, Yoshioka Y, Ohkawa A, Minowa K, Mukai Y, Abe Y, et al. Creation and X-ray structure analysis of the tumor necrosis factor receptor-1-selective mutant of a tumor necrosis factor-alpha antagonist. *J Biol Chem* 2008;283(2):998–1007.
- [25] Yamamoto Y, Tsutsumi Y, Yoshioka Y, Nishibata T, Kobayashi K, Okamoto T, et al. Site-specific PEGylation of a lysine-deficient TNF-alpha with full bioactivity. *Nat Biotechnol* 2003;21(5):546–52.
- [26] Abe Y, Yoshikawa T, Kamada H, Shibata H, Nomura T, Minowa K, et al. Simple and highly sensitive assay system for TNFR2-mediated soluble- and transmembrane-TNF activity. *J Immunol Methods* 2008;335(1–2):71–8.
- [27] Schwarz M, Rottgen P, Takada Y, Le Gall F, Knackmuss S, Bassler N, et al. Single-chain antibodies for the conformation-specific blockade of activated platelet integrin alphaIIb beta3 designed by subtractive selection from naive human phage libraries. *Faseb J* 2004;18(14):1704–6.
- [28] Popkov M, Rader C, Barbas 3rd CF. Isolation of human prostate cancer cell reactive antibodies using phage display technology. *J Immunol Methods* 2004; 291(1–2):137–51.
- [29] Eisenhardt SU, Schwarz M, Bassler N, Peter K. Subtractive single-chain antibody (scFv) phage-display: tailoring phage-display for high specificity against function-specific conformations of cell membrane molecules. *Nat Protoc* 2007;2(12):3063–73.
- [30] Shibata H, Yoshioka Y, Abe Y, Ohkawa A, Nomura T, Minowa K, et al. The treatment of established murine collagen-induced arthritis with a TNFR1-selective antagonistic mutant TNF. *Biomaterials* 2009;30(34):6638–47.
- [31] Shibata H, Yoshioka Y, Ikemizu S, Kobayashi K, Yamamoto Y, Mukai Y, et al. Functionalization of tumor necrosis factor-alpha using phage display technique and PEGylation improves its antitumor therapeutic window. *Clin Cancer Res* 2004;10(24):8293–300.
- [32] Wajant H, Pfizenmaier K, Scheurich P. Tumor necrosis factor signaling. *Cell Death Differ* 2003;10(1):45–65.
- [33] Weiss T, Grell M, Sieminski K, Muhlenbeck F, Durkop H, Pfizenmaier K, et al. TNFR80-dependent enhancement of TNFR60-induced cell death is mediated by TNFR-associated factor 2 and is specific for TNFR60. *J Immunol* 1998; 161(6):3136–42.
- [34] Fotin-Mlecsek M, Henkler F, Samel D, Reichwein M, Hausser A, Parmryd I, et al. Apoptotic crosstalk of TNF receptors: TNF-R2-induces depletion of TRAF2 and IAP proteins and accelerates TNF-R1-dependent activation of caspase-8. *J Cell Sci* 2002;115(Pt. 13):2757–70.
- [35] Yamagishi J, Kawashima H, Matsuo N, Ohue M, Yamayoshi M, Fukui T, et al. Mutational analysis of structure-activity relationships in human tumor necrosis factor-alpha. *Protein Eng* 1990;3(8):713–9.
- [36] Barbara JA, Smith WB, Gamble JR, Van Ostade X, Vandenabeele P, Tavernier J, et al. Dissociation of TNF-alpha cytotoxic and proinflammatory activities by p55 receptor- and p75 receptor-selective TNF-alpha mutants. *Embo J* 1994; 13(4):843–50.
- [37] Van Ostade X, Vandenabeele P, Everaerd B, Loetscher H, Gentz R, Brockhaus M, et al. Human TNF mutants with selective activity on the p55 receptor. *Nature* 1993;361(6409):266–9.
- [38] Loetscher H, Stueber D, Banner D, Mackay F, Lesslauer W. Human tumor necrosis factor alpha (TNF alpha) mutants with exclusive specificity for the 55-kDa or 75-kDa TNF receptors. *J Biol Chem* 1993;268(35):26350–7.
- [39] Abe Y, Nomura T, Yoshioka Y, Kamada H, Tsunoda S, Tsutsumi Y. Anti-inflammatory effects of a novel TNFR1-selective antagonistic TNF mutant on established murine collagen-induced arthritis. *Adv Exp Med Biol* 2011;691:493–500.
- [40] Yoshioka Y, Watanabe H, Morishige T, Yao X, Ikemizu S, Nagao C, et al. Creation of lysine-deficient mutant lymphotoxin-alpha with receptor selectivity by using a phage display system. *Biomaterials* 2010;31(7):1935–43.
- [41] Eck MJ, Sprang SR. The structure of tumor necrosis factor-alpha at 2.6 Å resolution. Implications for receptor binding. *J Biol Chem* 1989;264(29):17595–605.
- [42] Van Ostade X, Tavernier J, Fiers W. Structure-activity studies of human tumour necrosis factors. *Protein Eng* 1994;7(1):5–22.
- [43] Idriss HT, Naismith JH. TNF alpha and the TNF receptor superfamily: structure-function relationship(s). *Microsc Res Tech* 2000;50(3):184–95.
- [44] Mukai Y, Nakamura T, Yoshikawa M, Yoshioka Y, Tsunoda S, Nakagawa S, et al. Solution of the structure of the TNF-TNFR2 complex. *Sci Signal* 2010;3(148).ra83.



Annexin A4 is a possible biomarker for cisplatin susceptibility of malignant mesothelioma cells

Takuya Yamashita^{a,b,1}, Kazuya Nagano^{a,1}, So-ichiro Kanasaki^{a,b}, Yuka Maeda^{a,b}, Takeshi Furuya^{a,b}, Masaki Inoue^a, Hiromi Nabeshi^b, Tomoaki Yoshikawa^{a,b}, Yasuo Yoshioka^{a,b,c}, Norio Itoh^b, Yasuhiro Abe^a, Haruhiko Kamada^{a,c}, Yasuo Tsutsumi^{a,b,c}, Shin-ichi Tsunoda^{a,c,d,*}

^a Laboratory of Biopharmaceutical Research, National Institute of Biomedical Innovation, 7-6-8 Saito-Asagi, Ibaraki, Osaka 567-0085, Japan

^b Laboratory of Toxicology and Safety Science, Graduate School of Pharmaceutical Sciences, Osaka University, 1-6 Yamadaoka, Suita, Osaka 565-0871, Japan

^c The Center for Advanced Medical Engineering and Informatics, Osaka University, 1-6 Yamadaoka, Suita, Osaka 565-0871, Japan

^d Laboratory of Biomedical Innovation, Graduate School of Pharmaceutical Sciences, Osaka University, 1-6 Yamadaoka, Suita, Osaka 565-0871, Japan

ARTICLE INFO

Article history:

Received 27 March 2012

Available online 4 April 2012

Keywords:

Malignant mesothelioma

Cisplatin susceptibility

Annexin A4

Biomarker

Proteomics

ABSTRACT

Mesothelioma is a highly malignant tumor with a poor prognosis and limited treatment options. Although cisplatin (CDDP) is an effective anticancer drug, its response rate is only 20%. Therefore, discovery of biomarkers is desirable to distinguish the CDDP-susceptible versus resistant cases. To this end, differential proteome analysis was performed to distinguish between mesothelioma cells of different CDDP susceptibilities, and this revealed that expression of annexin A4 (ANXA4) protein was higher in CDDP-resistant cells than in CDDP-susceptible cells. Furthermore, ANXA4 expression levels were higher in human clinical malignant mesothelioma tissues than in benign mesothelioma and normal mesothelial tissues. Finally, increased susceptibility was observed following gene knockdown of ANXA4 in mesothelioma cells, whereas the opposite effect was observed following transfection of an ANXA4 plasmid. These results suggest that ANXA4 has a regulatory function related to the cisplatin susceptibility of mesothelioma cells and that it could be a biomarker for CDDP susceptibility in pathological diagnoses.

© 2012 Elsevier Inc. All rights reserved.

1. Introduction

Malignant mesothelioma is an aggressive neoplasm located on serosal membrane surfaces such as the pleura, and less frequently the peritoneum, and it has a poor outcome. The five-year survival rate is only about 5%. On the other hand, it is well known that asbestos is the major causative agent in the development of this disease [1–3]. Moreover, malignant mesothelioma takes 40–50 years to develop following exposure to asbestos. Because of its adiabatic potential, asbestos was commonly used as a building material in the 1960–1970s. Thus, an increase in mesothelioma patients is expected in the future. Patients with pleural malignant mesothelioma commonly present with an effusion associated with breathlessness that is often accompanied by chest-wall pain and a cough. After confirming the diagnosis, many patients are treated by intensive multidirectional approaches that combine cytoreductive surgery with intrapleural or intraperitoneal chemotherapy [4–8]. However, cytoreductive surgery is not always possible for pa-

tients with extensive intraperitoneal disease. Thus, the role of chemotherapy in malignant mesothelioma is critically important.

CDDP is an extensively used anticancer drug for the treatment of malignant mesothelioma, although the response rate is only about 20% [9–12]. A major problem with CDDP treatment of malignant mesothelioma patients is the development of CDDP insusceptibility. Thus, there is an urgent need to further our understanding of the pathogenesis of malignant mesothelioma, particularly with respect to the expression of proteins that confer drug susceptibility, in order to develop novel therapeutic strategies. In this study, a proteomic analysis was performed using high- and low-CDDP-susceptible malignant mesothelioma cells to identify candidate proteins associated with CDDP susceptibility.

2. Materials and methods

2.1. Cells

H28, H2052, H2452, H226 and MSTO-221H were purchased from American Type Culture Collection and maintained in RPMI1640 medium (Wako) containing 10% fetal calf serum (Biowest). Human mesothelial cells (HMC) were purchased from

* Corresponding author at: Laboratory of Biopharmaceutical Research, National Institute of Biomedical Innovation, 7-6-8 Saito-Asagi, Ibaraki, Osaka 567-0085, Japan. Fax: +81 72 641 9817.

E-mail address: tsunoda@nibio.go.jp (S.-i. Tsunoda).

¹ These authors contributed equally to this work.

Sciencell and cultured in Mesothelial Cell Growth Medium (Zen-Bio) under a 5% CO₂ atmosphere at 37 °C.

2.2. Measurement of cisplatin susceptibility in malignant mesothelioma cells

Malignant mesothelioma cells were seeded into 96-well microplates and cultured overnight. Various concentrations of CDDP were added to each well, the plates were incubated for 24 h, and cell viability was measured using Cell count reagent SF (Nacal Tesque). Absorbance was measured using a microplate reader (Bio-Rad) at test and reference wavelengths of 450 and 650 nm, respectively.

2.3. Proteomic analysis using two dimensional differential in-gel electrophoresis

For proteomic analysis, quantitative analysis was performed using two dimensional differential in-gel electrophoresis (2D-DIGE). Cell lysates were prepared from H28 and H2052 and then solubilized with 7 M urea, 2 M thiourea, 4% CHAPS and 10 mM Tris-HCl (pH 8.5). The lysates were labeled at the ratio of 50 µg proteins: 400 pmol Cy3 or Cy5 protein-labeling dye (GE Healthcare Biosciences) in dimethylformamide according to the manufacturer's protocol. The labelled samples were mixed with rehydration buffer (7 M urea, 2 M thiourea, 4% CHAPS, 2% DTT, 2% Pharmalyte (GE Healthcare Biosciences)) and applied to a 24-cm immobilized pH gradient gel strip (IPG-strip pH 4–7) for separation in the first dimension. For the second dimension separation, the IPG-strips were treated with iodoacetamide and applied to SDS-PAGE gels (10% polyacrylamide and 2.7% *N,N'*-diallyltartardiamide gels). After electrophoresis, the gels were scanned with a laser fluorimager (Typhoon Trio, GE Healthcare Biosciences). The spot-picking gel was scanned after staining with Deep purple total protein stain (GE Healthcare Biosciences). Quantitative analysis of protein spots was carried out with Decyder-DIA software (GE Healthcare Biosciences). For the antigen spots of interest, spots of 1 mm × 1 mm in size were picked using Ettan Spot Picker (GE Healthcare Biosciences).

2.4. In-gel tryptic digestion

Picked gel pieces were destained with 50% acetonitrile/50 mM NH₄HCO₃ for 20 min twice, dehydrated with 75% acetonitrile for 20 min, and then dried using a centrifugal concentrator. Five microliter of 20 µg/ml trypsin (Promega) solution was added to each gel piece and the pieces were incubated for 16 h at 37 °C. The digested peptides were extracted sequentially using 50%, 80%, and 100% acetonitrile and then dried before being suspended in 10 µl of 0.1% formic acid.

2.5. Mass spectrometry and database search

Extracted peptides were analyzed by liquid chromatography ultra high resolution time-of-flight mass spectrometry (LC-UHR TOF-MS/MS; maXis, Bruker Daltonics). The Mascot search engine (<http://www.matrixscience.com>) was initially used to query the entire theoretical tryptic peptide database as well as SwissProt (<http://www.expasy.org/>, a public domain database provided by the Swiss Institute of Bioinformatics). The search query assumed the following: (i) the peptides were mono-, di- or tri-isotopic, (ii) methionine residues may be oxidized, (iii) all cysteines were modified with carbamidomethyl.

2.6. Western blot

The cell lysates were separated in 10% SDS-polyacrylamide gels and transferred to Immobilon membranes (Millipore). After blocking by 4% block ace (DS Pharma Biomedical) for 1 h at room temperature, the blots were reacted with primary antibodies in a buffer containing 0.4% block ace, and then with the appropriate peroxidase-conjugated secondary antibodies in the same buffer. Expression of ANXA4 in malignant mesothelioma cells was detected by mouse anti-human ANXA4 (Abnova: 1D3) followed by an HRP-conjugated anti-mouse IgG antibody (Sigma-Aldrich) using the ECL-plus system (GE Healthcare Biosciences). Equal amounts of protein loading were confirmed by parallel β-actin immunoblotting, and signal quantification was performed by densitometric scanning.

2.7. Immunohistochemistry staining

Human mesothelioma and normal tissue sections were deparaffinated in xylene and rehydrated in a graded series of ethanol dilutions. Heat-induced epitope retrieval was performed by incubating at different temperatures following the manufacturer's instructions using Target Retrieval Solution pH 9 (Dako). After heat-induced epitope retrieval treatment, endogenous peroxidase was blocked with a peroxidase blocking reagent (Dako). Following peroxidase blocking, the slides were incubated with 10% bovine serum albumin (BSA) solution for 30 min at room temperature. The slides were then incubated for 60 min with anti-human ANXA4 monoclonal antibody (9 µg/ml) in 3% BSA at room temperature. After washing 3 times with wash buffer (Dako), the slides were incubated for 30 min with ENVISION + Dual Link (Dako) at room temperature. They were then washed final 3 times and stained with 3,3'-diaminobenzidine. After development, the slides were lightly counterstained with Mayer's hematoxylin and mounted with resinous mounting medium.

2.8. Cisplatin susceptibility in cells transfected with ANXA4-siRNA and ANXA4-plasmid

H28 was transfected with ANXA4-siRNA (target sequence: AAGGATATCACAGAAGGATAT, Qiagen) using Hyperfect reagent (Qiagen) according to the manufacturer's instructions. In contrast, H2052 was transfected with ANXA4-pcDNA 3.1 (a gift from Naka T: Laboratory for Immune Signal, National Institute of Biomedical Innovation) using FuGENE HD transfection reagent (Roche). After transfection, the cells were treated with various concentrations of CDDP for 36 h (ANXA4-siRNA) or 24 h (ANXA4-pcDNA 3.1). Cell viability was measured as described above.

2.9. Statistical analysis

Differences in tumor volumes between the control and target groups were compared using the unpaired Student's *t*-test.

3. Results

3.1. CDDP susceptibility in malignant mesothelioma cells

Cell viability following CDDP treatment was examined to determine which cell lines had higher or lower susceptibility to CDDP. Among five tested mesothelioma cell lines, H2052 was the most and H28 the least susceptible cell line (Fig. 1). The IC₅₀ values of H28, H2052, H2452, H226 and MSTO-221H were 154.5, 27.8, 66.0, 87.5 and 49.5 µM, respectively.

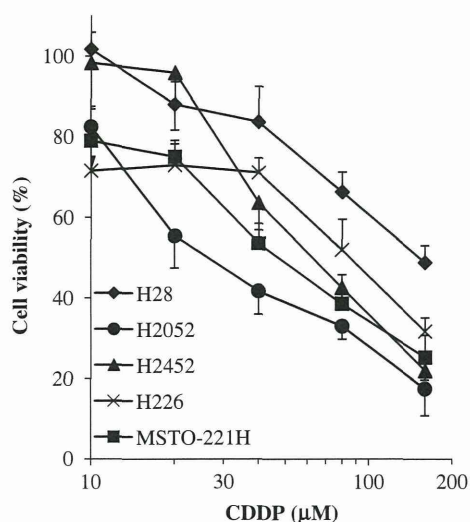


Fig. 1. Susceptibility of malignant mesothelioma cells to CDDP. Mesothelioma cells, H28, H2052, H2452, H226 and MSTO-221H were cultured with various concentrations of CDDP for 24 h 37 °C under 5% CO₂. Cell viability was assayed using the WST-8 assay. Maximal cell viability (100%) was obtained by incubating cells without CDDP. Data are shown as means and standard deviations ($n = 4$).

3.2. Identification of differentially expressed proteins by 2D-DIGE and MS

In order to search for CDDP susceptibility-related proteins, differential proteome analysis between H2052 and H28 cell lines was performed to search for CDDP susceptibility-related proteins (Fig. 2). Quantitative image analysis indicated that a total of eight protein spots representing > 2.0-fold alteration in expression were found and then identified by MS analysis (Table 1). Among those eight proteins, we focused on ANXA4 because this protein plays an important role in membrane stability. Previous reports have indicated that ANXA4 is associated with chemoresistance against platinum-based anticancer drugs in human lung, colon [13] and ovarian cancer [14].

3.3. ANXA4 expression analysis in human malignant mesothelioma cells and mesothelial tissues

Correlations between the expression levels in five malignant mesothelioma cell lines with CDDP-susceptibility were examined using western blot analysis to validate the identified proteins as CDDP susceptibility-related proteins. ANXA4 was expressed at a higher level in H28 cells relative to the other four CDDP-susceptible malignant mesothelioma cell lines (Fig. 3A and B). Expression of ANXA4 in human mesothelial tissue was analyzed by immunohistochemistry staining with an anti-human ANXA4 monoclonal antibody. Fig. 3C indicates that ANXA4 was expressed at higher levels in human malignant mesothelioma tissues than in benign mesothelioma tissues and normal mesothelial tissues.

3.4. Gene regulation of ANXA4 in malignant mesothelioma cells by knockdown and overexpression

ANXA4-siRNA and ANXA4-pcDNA 3.1 were next transfected to H28 and H2052 before CDDP treatment to evaluate correlations between ANXA4 expression levels and CDDP susceptibility. The IC₅₀ values of [H28/non treat: H28/control-siRNA: H28/ANXA4-siRNA] were [80.0 μM: 71.8 μM: 15.5 μM] and [H2052/control-pcDNA 3.1: [H2052/ANXA4-pcDNA 3.1] were [55.2 μM: 89.7 μM], respectively (Fig. 4A–D). These results suggested that the CDDP susceptibility of H28 cells was increased by ANXA4-siRNA transfection and that of H2052 cells was decreased by ANXA4-pcDNA 3.1 transfection.

4. Discussion

In this study, a proteomic analysis was performed based on 2D-DIGE using malignant mesothelioma cell lines to identify candidate proteins associated with CDDP susceptibility (Figs. 1 and 2). Eight proteins that were differentially expressed in H28 cells compared with H2052 cells were identified (Table 1). ANXA4 was found to be expressed at a higher level in H28 cells relative to levels in CDDP-susceptible malignant mesothelioma cells by western blot

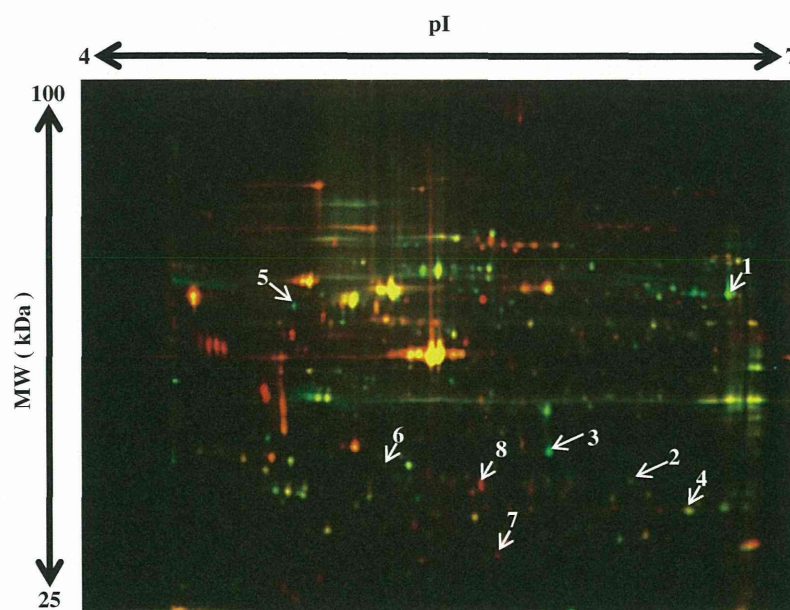


Fig. 2. 2D-DIGE image of fluorescently labeled proteins from human mesothelioma cell lines H28 and H2052. Proteins from high- and low-susceptible mesothelioma cells (H2052, H28) were labeled with cy3 and cy5, respectively, and 2D electrophoresis was performed. The differentially expressed spots in H28 indicated by white arrows were then identified by LC-TOF-MS/MS. Table 1 contains additional information about the identified proteins.

Table 1
Proteins expressed at higher or lower levels in H28 compared to H2052.

No.	Accession number	Protein name	pI	MW (kDa)	Expression ratio (H28/H2052)
1	P11413	Glucose-6-phosphate 1-dehydrogenase	6.4	59.3	21.0
2	P78417	Glutathione S-transferase omega-1	6.2	27.6	7.4
3	P09525	Annexin A4	5.6	35.9	3.6
4	P30041	Peroxiredoxin-6	6.0	25.0	3.5
5	Q09028	Histone-binding protein RBBP4	4.7	47.7	3.0
6	P07195	L-lactate dehydrogenase B chain	5.7	36.6	2.9
7	P32119	Peroxiredoxin-2	5.7	21.9	0.03
8	Q9Y696	Chloride intracellular channel protein 4	5.5	28.8	0.13

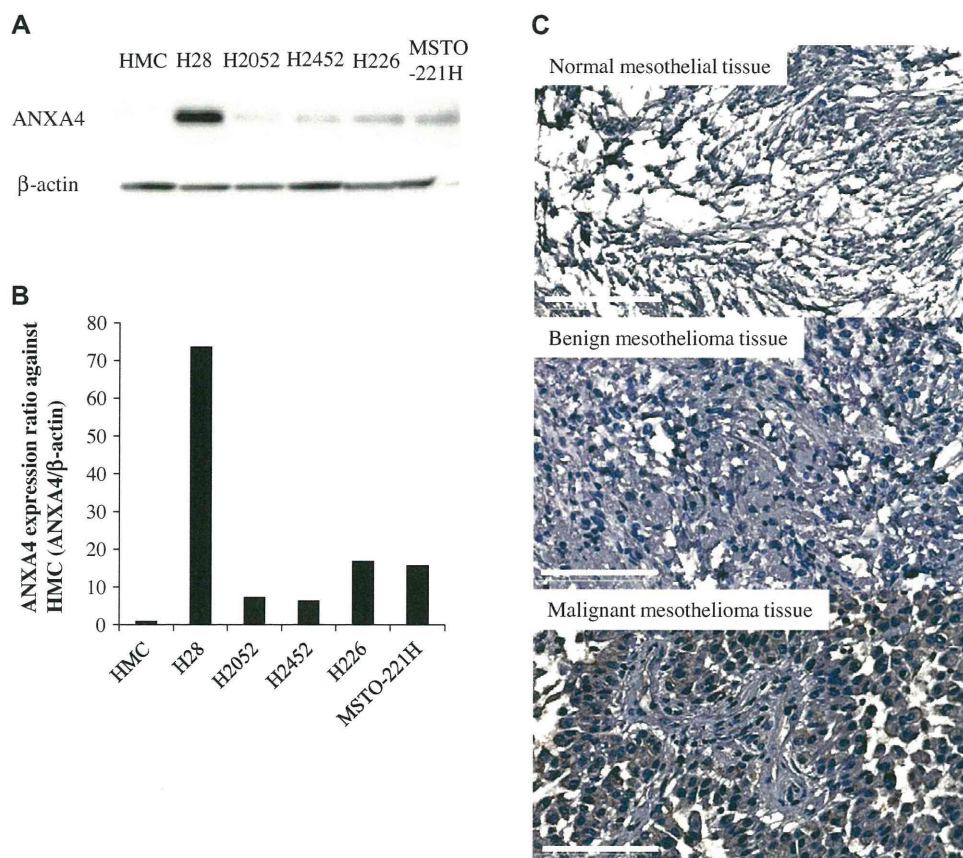


Fig. 3. ANXA4 expression analysis in human malignant mesothelioma cells and mesothelial tissues. ANXA4 expression levels in human primary mesothelial cells, HMC, and mesothelioma cell lines (H28, H2052, H2452, H226, MSTO-221H) were analyzed by western blotting (A). Intensity of the western blotting images was quantified by densitometry (B). Expression of ANXA4 in human mesothelial tissues was analyzed by immunostaining using an anti-human ANXA4 antibody (C). Top, middle and bottom panels are normal mesothelial, benign and malignant mesothelioma tissues, respectively. The tissue sections were counterstained using hematoxylin. Representative 400 \times photomicrographs presented (bar: 100 μ m).

analysis (Fig. 3A and B). Furthermore, ANXA4 was expressed in malignant mesothelioma tissue but not in benign mesothelial tumor and normal mesothelial tissues (Fig. 3C). Thus, ANXA4 was expressed in CDDP-susceptible malignant mesothelioma cells and specifically in malignant mesothelioma tissues. These results indicate that ANXA4 expression in malignant mesothelioma cells may be correlated with CDDP susceptibility, although this relationship must be validated in future studies of human clinical malignant mesothelial cases. The CDDP susceptibility of H28 cells was actually increased by ANXA4 knockdown, and that of H2052 cells was decreased by ANXA4 overexpression (Fig. 4). Thus, these results suggest that ANXA4 plays an important role in chemoresistance against CDDP.

ANXA4 has already been characterized as a regulator of cell membranes with calcium dependency [15–17]. Recently, some studies have reported the protein is associated with membrane

permeability [18], ion channels [19] and exocytosis [20,21]. These observations may explain in part the correlation of ANXA4 with modulation of drug susceptibility in cancer cells.

This study demonstrates for the first time elevated ANXA4 protein expression in malignant mesothelioma cells that have less susceptibility to CDDP. *In vitro* evaluation of drug susceptibility against CDDP in malignant mesothelioma cells derived from cancer patients would be important in clinical conditions because doctors as well as patients wish to avoid treatment with inefficacious drugs. Consequently, the susceptibility of a given patient against CDDP could be confirmed by analyzing the expression level of ANXA4 in malignant mesothelioma patients at the time of diagnosis. Furthermore, if ANXA4 expression could be blocked specifically in malignant mesothelioma cells by nucleic acid drugs such as siRNA, this procedure would prove useful in clinical situations involving CDDP treatment. The present study may contribute to

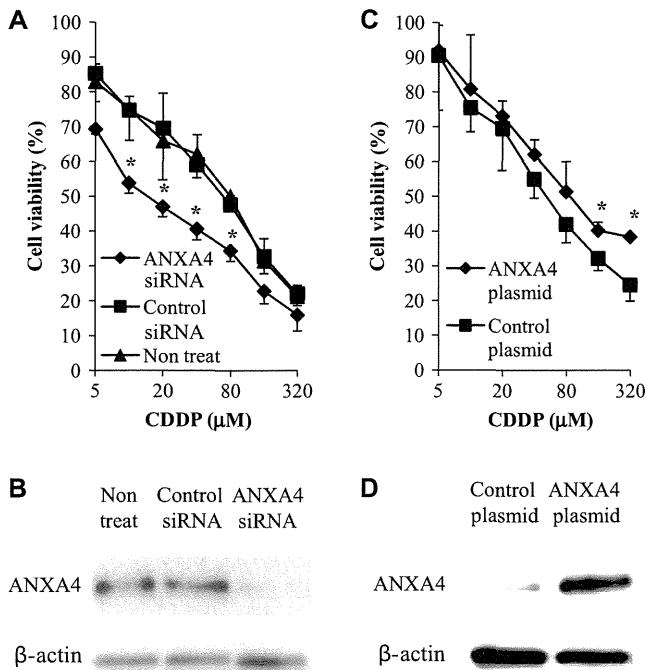


Fig. 4. The effect of ANXA4 gene knockdown and overexpression on CDDP susceptibility in malignant mesothelioma cells. Transfection of ANXA4 siRNA or plasmid into malignant mesothelioma cells confers resistance to CDDP. Cell survival after 24 h treatment of H28/ANXA4 siRNA or H2052/ANXA4 plasmid with different concentrations of CDDP (A and C). Expression of ANXA4 was analyzed by western blot analysis (B and D). Data are shown as means and standard deviations ($n = 4$). * $P < 0.05$ (Control siRNA or plasmid vs. ANXA4 siRNA or plasmid).

establishment of a new therapeutic strategy for malignant mesothelioma patients by suggesting a novel diagnostic and therapeutic target.

Acknowledgments

This study was supported in part by Grants-in-Aid for Scientific Research from the Ministry of Education, Culture, Sports, Science and Technology of Japan, and from the Japan Society for the Promotion of Science (JSPS). This study was also supported in part by Health Labor Sciences Research Grants from the Ministry of Health, Labor and Welfare of Japan and by Health Sciences Research Grants for Research on Publicly Essential Drugs and Medical Devices from the Japan Health Sciences Foundation.

References

- [1] W.N. Rom, W.D. Travis, A.R. Brody, Cellular and molecular basis of the asbestos-related diseases, *Am. Rev. Respir. Dis.* 143 (1991) 408–422.

- [2] N.H. Heintz, Y.M. Janssen-Heininger, B.T. Mossman, Asbestos, lung cancers, and mesotheliomas: from molecular approaches to targeting tumor survival pathways, *Am. J. Respir. Cell Mol. Biol.* 42 (2010) 133–139.
- [3] Consensus Report: Asbestos, asbestosis, and cancer: the Helsinki criteria for diagnosis and attribution. *Scand. J. Work Environ. Health* 23 (1997) 311–316.
- [4] T.D. Yan, L. Welch, D. Black, P.H. Sugarbaker, A systematic review on the efficacy of cytoreductive surgery combined with perioperative intraperitoneal chemotherapy for diffuse malignancy peritoneal mesothelioma, *Ann. Oncol.* 18 (2007) 827–834.
- [5] E. Chailleux, D. Pioche, S. Chopra, G. Dabouis, P. Germaud, A.Y. De Lajartre, M. De Lajartre, Prognostic factors in diffuse malignant pleural mesothelioma: a study of 167 patients, *Chest* 93 (1988) 159–162.
- [6] K.S. Sridhar, R. Doria, W.A. Raub Jr., R.J. Thurer, M. Saldana, New strategies are needed in diffuse malignant mesothelioma, *Cancer* 70 (1992) 2969–2979.
- [7] M. Markman, D. Kelsen, Efficacy of cisplatin-based intraperitoneal chemotherapy as treatment of malignant peritoneal mesothelioma, *J. Cancer Res. Clin. Oncol.* 118 (1992) 547–550.
- [8] G.H. Eltabakh, M.S. Piver, R.E. Hempling, F.O. Recio, M.E. Intengen, Clinical picture, response to therapy, and survival of women with diffuse malignant peritoneal mesothelioma, *J. Surg. Oncol.* 70 (1999) 6–12.
- [9] T. Berghmans, M. Paesmans, Y. Lalami, I. Louviaux, S. Luce, C. Mascaux, A.P. Meert, J.P. Sculier, Activity of chemotherapy and immunotherapy on malignant mesothelioma: a systematic review of the literature with meta-analysis, *Lung. Cancer* 38 (2002) 111–121.
- [10] H.J. Lerner, D.A. Schoenfeld, A. Martin, G. Falkson, E. Borden, Malignant mesothelioma: The Eastern Cooperative Oncology Group (ECOG) experience, *Cancer* 52 (1983) 1981–1985.
- [11] D.M. Mintzer, D. Kelsen, D. Frimmer, R. Heelan, R. Gralla, Phase II trial of high-dose cisplatin in patients with malignant mesothelioma, *Cancer Treat Rep.* 69 (1985) 711–712.
- [12] B.L. Zidar, S. Green, H.I. Pierce, R.W. Roach, S.P. Balcerzak, L. Militello, A phase II evaluation of cisplatin in unresectable diffuse malignant mesothelioma: a Southwest Oncology Group Study, *Invest New Drugs* 6 (1988) 223–226.
- [13] E.K. Han, S.K. Tahir, S.P. Cherian, N. Collins, S.C. Ng, Modulation of paclitaxel resistance by annexin IV in human cancer cell lines, *Br. J. Cancer* 83 (2000) 83–88.
- [14] A. Kim, T. Enomoto, S. Serada, Y. Ueda, T. Takahashi, B. Ripley, T. Miyatake, M. Fujita, C.M. Lee, K. Morimoto, M. Fujimoto, T. Kimura, T. Naka, Enhanced expression of Annexin A4 in clear cell carcinoma of the ovary and its association with chemoresistance to carboplatin, *Int. J. Cancer* 125 (2009) 2316–2322.
- [15] M.A. Kaetzel, P. Hazarika, J.R. Dedman, Differential tissue expression of three 35-kDa annexin calcium-dependent phospholipid-binding proteins, *J. Biol. Chem.* 264 (1989) 14463–14470.
- [16] G. Zanotti, G. Malpeli, F. Gliubich, C. Folli, M. Stoppini, L. Olivi, A. Savoia, R. Berni, Structure of the trigonal crystal form of bovine annexin IV, *Biochem. J.* 329 (1998) 101–106.
- [17] M.A. Kaetzel, Y.D. Mo, T.R. Mealy, B. Campos, W. Bergsma-Schutter, A. Brisson, J.R. Dedman, B.A. Seaton, Phosphorylation mutants elucidate the mechanism of annexin IV-mediated membrane aggregation, *Biochemistry* 40 (2001) 4192–4199.
- [18] W.G. Hill, M.A. Kaetzel, B.K. Kishore, J.R. Dedman, M.L. Zeidel, Annexin A4 reduces water and proton permeability of model membranes but does not alter aquaporin 2-mediated water transport in isolated endosomes, *J. Gen. Physiol.* 121 (2003) 413–425.
- [19] M.A. Kaetzel, H.C. Chan, W.P. Dubinsky, J.R. Dedman, D.J. Nelson, A role for annexin IV in epithelial cell function. Inhibition of calcium-activated chloride conductance, *J. Biol. Chem.* 269 (1994) 5297–5302.
- [20] H. Sohma, C.E. Creutz, S. Gasa, H. Ohkawa, T. Akino, Y. Kuroki, Differential lipid specificities of the repeated domains of annexin IV, *Biochim. Biophys. Acta* 1546 (2001) 205–215.
- [21] A. Piljic, C. Schultz, Annexin A4 self-association modulates general membrane protein mobility in living cells, *Mol. Biol. Cell* 17 (2006) 3318–3328.

Laboratory of Biopharmaceutical Research¹, National Institute of Biomedical Innovation; Laboratory of Toxicology and Safety Science², Graduate School of Pharmaceutical Sciences; The Center for Advanced Medical Engineering and Informatics³; Laboratory of Biomedical Innovation⁴, Graduate School of Pharmaceutical Sciences, Osaka University, Osaka, Japan

Rho GDP-dissociation inhibitor alpha is associated with cancer metastasis in colon and prostate cancer

T. YAMASHITA^{1,2,*}, T. OKAMURA^{1,*}, K. NAGANO^{1,*}, S. IMAI¹, Y. ABE¹, H. NABESHI^{1,2}, T. YOSHIKAWA^{1,2}, Y. YOSHIOKA^{1,2,3}, H. KAMADA^{1,3}, Y. TSUTSUMI^{1,2,3}, S. TSUNODA^{1,3,4}

Received July 7, 2011, accepted August 5, 2011

Shin-ichi Tsunoda, Ph.D, Laboratory of Biopharmaceutical Research, National Institute of Biomedical Innovation, 7-6-8 Saito-Asagi, Ibaraki, Osaka 567-0085, Japan.

tsunoda@nibio.go.jp

*These authors contributed equally to the work.

Pharmazie 67: 253–255 (2012)

doi: 10.1691/ph.2012.1630

Since metastasis is one of the most important prognostic factors in colorectal cancer, development of new methods to diagnose and prevent metastasis is highly desirable. However, the molecular mechanisms leading to the metastatic phenotype have not been well elucidated. In this study, a proteomics-based search was carried out for metastasis-related proteins in colorectal cancer by analyzing the differential expression of proteins in primary versus metastasis focus-derived colorectal tumor cells. Protein expression profiles were determined using a tissue microarray (TMA), and the results identified Rho GDP-dissociation inhibitor alpha (Rho GDI) as a metastasis-related protein in colon and prostate cancer patients. Consequently, Rho GDI may be useful as a diagnostic biomarker and/or a therapeutic to prevent colon and prostate cancer metastasis.

1. Introduction

Colorectal cancer is known as a major metastatic cancer, and 40–50% of patients already have a metastatic focus at presentation. Moreover, the 5-year survival of these patients is under 10% (Davies et al. 2005). Thus, metastasis is one of the most important prognostic factors in colorectal cancer. In order to improve rates of cancer remission, it will be necessary to clarify the detailed molecular mechanisms of cancer metastasis and to utilize this information to establish new diagnostic and therapeutic techniques. Many researchers have searched for metastasis-related molecules (Liu et al. 2010; Shuehara et al. 2011) using proteomics techniques (Hanash 2003). Comprehensive mapping of the molecular changes during metastasis would greatly improve our understanding of the recurrence and management of cancer. However, the knowledge gained so far in these studies has not been sufficient to improve cancer remission rates.

Here we show the potential of Rho GDI as a metastasis-related protein in colon and prostate cancer patients. In order to identify metastasis-related proteins, the protein expression patterns of human colorectal cancer cells with different metastatic characters were compared. Because these cells were derived from the same patient (SW480: a surgical specimen of a primary colon adenocarcinoma, SW620: a lymph node metastatic focus), cancer metastasis-related protein candidates could be effectively sought without background variations due to differences between individuals. Furthermore, by analyzing the expression of candidate proteins in many clinical samples using a TMA, we attempted to validate the association of these candidates

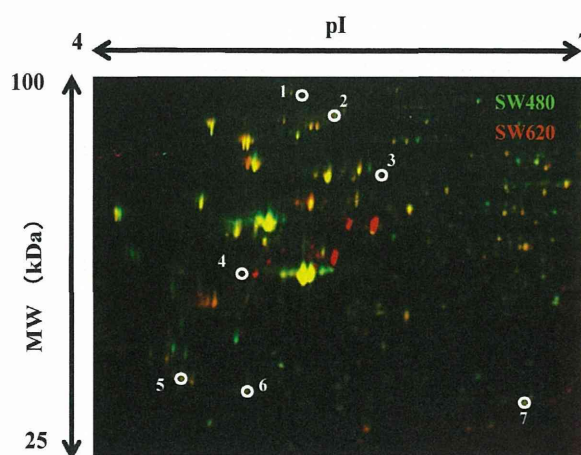


Fig. 1: 2D-DIGE image of fluorescently-labeled proteins from different metastatic human colorectal cancer cells. SW480 is human colorectal cancer cell line derived from a primary tumor and SW620 is derived from a metastatic focus from the same patient. Proteins from the colon cancer cells (SW480, SW620) were labeled with Cy3 and Cy5 respectively, and analyzed by 2D electrophoresis. The differentially-expressed spots (white circles) were then identified by LC-UHR TOF/MS

with metastasis. TMA is a slide glass containing many clinical tissues, and it enables one to carry out a high-throughput analysis by evaluating the relationship between expression profiles of each candidate molecule and clinical information such as metastasis. (Imai et al. 2011; Yoshida et al. 2011).

Table 1: High expression proteins in SW620 compared to SW480

	Accession	Protein name	MW (kDa)	pI	Ratio (SW620 / SW480)
1	P12109	collagen alpha-1(VI) chain	108.6	5.3	1.53
2	Q15459	splicing factor 3A subunit 1	88.9	5.2	1.61
3	P13797	T-plastin	70.9	5.5	1.59
4	P60709	actin cytoplasmic 1	42.1	5.3	1.50
5	P63104	14-3-3 zeta/delta	27.9	4.7	1.63
6	P52565	Rho GDP-dissociation inhibitor 1 (Rho GDI)	23.3	5.0	1.90
7	P30041	Peroxiredoxin-6 (PRDX6)	25.1	6.0	1.86

2. Investigations, results and discussion

In order to search for metastasis-related proteins, we analyzed differentially-expressed proteins between SW480 and SW620 by two-dimensional differential in-gel electrophoresis (2D-DIGE) (Fig. 1). As a result, 7 spots with at least a 1.5-fold-altered expression level were found by quantitative analysis, and these spots were identified by mass spectrometry (Table 1). Three molecules having a high SW620/SW480 expression ratio indicating a strong association with cancer metastasis were identified: Rho GDP-dissociation inhibitor alpha (Rho GDI), peroxiredoxin-6 (PRDX6) and 14-3-3 zeta/delta.

The expression profiles of these proteins were analyzed by immunohistochemistry using the TMA with colon cancer and multiple cancer tissues. Results of this analysis indicated that expression of PRDX6 and 14-3-3 zeta/delta had no relationship to the clinical status of cancer metastasis (data not shown). On the other hand, in positive cases of lymph node metastasis, the expression ratio of Rho GDI was significantly higher than in the negative cases. Furthermore, the same trend was seen when tissues from prostate cancer patients were analyzed (Table 2). To confirm these results, the expression levels of Rho GDI protein in colon cancer cell lines with different metastatic potential (SW480 < SW620 < SW620-OK1 < SW620-OK2: Characteristics of SW620-OK1 and SW620-OK2 are described in *Experimental*) were investigated by western blot analysis (Fig. 2). The expression of Rho GDI was found to be up-regulated with the development of metastatic characteristics. These results suggested that Rho GDI is correlated with cancer metastasis.

Rho GDI has been identified as key regulator of Rho family GTPases. Activation of growth factor receptors and integrins can promote the exchange of GDP for GTP on Rho proteins (Bishop et al. 2000). Furthermore, GTP-bound Rho proteins interact with a range of effector molecules to modulate their activity or localization, and this leads to changes in cell behavior. It is clear that Rho family GTPases are involved in the control of cell morphology and motility (Etienne-Manneville et al. 2002; Hall et al. 1997; Van Aelst et al. 1997). The importance of Rho protein and Rho GDI in cancer progression, particularly in the area of metastasis, is becoming increasingly evident. Recently, some reports have indicated that the expression of Rho GDI was correlated with colorectal and breast cancer metastasis (Zhao et al. 2008; Kang et al. 2010). Thus, our findings are consistent with these reports and further suggest that the expression of Rho GDI is also correlated with prostate cancer metastasis. Consequently, Rho GDI should be considered as a diagnostic marker or new therapeutic target for cancer metastasis.

3. Experimental

3.1. Cell lines

SW480 is a human colorectal cancer cell line derived from a primary focus and SW620 is derived from a metastatic focus of the same patient. These

cells were purchased from American Type Culture Collection and maintained at 37 °C using Leibovitz's L-15 medium (Wako) supplemented with 10% FCS. SW620-OK1 and -OK2 were established by the following procedure: 1×10^6 SW620 cells were injected into the spleens of nu/nu mice. After 8 weeks, SW620-OK1 was established from a liver metastatic focus. Furthermore, SW620-OK2 was established from SW620-OK1 using the same procedures.

3.2. 2D-DIGE analysis

Cell lysates were prepared from SW480 and SW620 and then solubilized with 7 M urea, 2 M thiourea, 4% CHAPS and 10 mM Tris-HCl (pH 8.5). The lysates were labeled at the ratio of 50 µg proteins: 400 pmol Cy3 or Cy5 protein-labeling dye (GE Healthcare Biosciences) in dimethylformamide according to the manufacturer's protocol. Briefly, the labelled samples were mixed with rehydration buffer (7 M urea, 2 M thiourea, 4% CHAPS, 2% DTT, 2% Pharmalyte (GE Healthcare Biosciences)) and applied to a 24-cm immobilized pH gradient gel strip (IPG-strip pH 4–7 NL) for separation in the first dimension. Samples for the spot-picking gel were prepared without labelling by Cy-dyes. For the second dimension separation, the IPG-strips were applied to SDS-PAGE gels (10% polyacrylamide and 2.7% N,N'-diallyltartardiamide gels). After electrophoresis, the gels were scanned with a laser fluorimeter (Typhoon Trio, GE Healthcare Biosciences). The spot-picking gel was scanned after staining with Deep Purple Total Protein Stain (GE Healthcare Biosciences). Quantitative analysis of protein spots was carried out with Decyder-DIA software (GE Healthcare Biosciences). For the antigen spots of interest, spots of 1 mm × 1 mm in size were picked using Ettan Spot Picker (GE Healthcare Biosciences).

3.3. In-gel tryptic digestion

Picked gel pieces were digested with trypsin as described below. The gel pieces were destained with 50% acetonitrile/50 mM NH_4HCO_3 for 20 min twice, dehydrated with 75% acetonitrile for 20 min, and then dried using a centrifugal concentrator. Next, 5 µl of 20 µl/ml trypsin (Promega) solution was added to each gel piece and incubated for 16 h at 37 °C. Three solutions were used to extract the resulting peptide mixtures from the gel pieces. First, 50 µl of 50% (v/v) acetonitrile in 0.1% (v/v) formic acid (FA) was added to the gel pieces, which were then sonicated for 5 min. Next, we collected the solution and added 80% (v/v) acetonitrile in 0.1% FA. Finally, 100% acetonitrile was added for the last extraction. The peptides were dried and then re-suspended in 10 µl of 0.1% FA.

3.4. Mass spectrometry and database search

Extracted peptides were analyzed by liquid chromatography Ultra High Resolution time-of-flight mass spectrometry (LC-UHR TOF/MS; maXis, Bruker Daltonics). The Mascot search engine (<http://www.matrixscience.com>) was initially used to query the entire theoretical tryptic peptide database as well as SwissProt (<http://www.expasy.org/>), a public domain database pro-

Table 2: Expression profile of Rho GDI in primary cancers with or without lymph node metastasis

	Number of Rho GDI positive cases (positive ratio)	
	in metastasis negative cases	in metastasis positive cases
Colon cancer*	11/14 (79%)	19/19 (100%)
Prostate cancer*	18/23 (78%)	11/11 (100%)

* $p < 0.05$: Mann Whitney U test

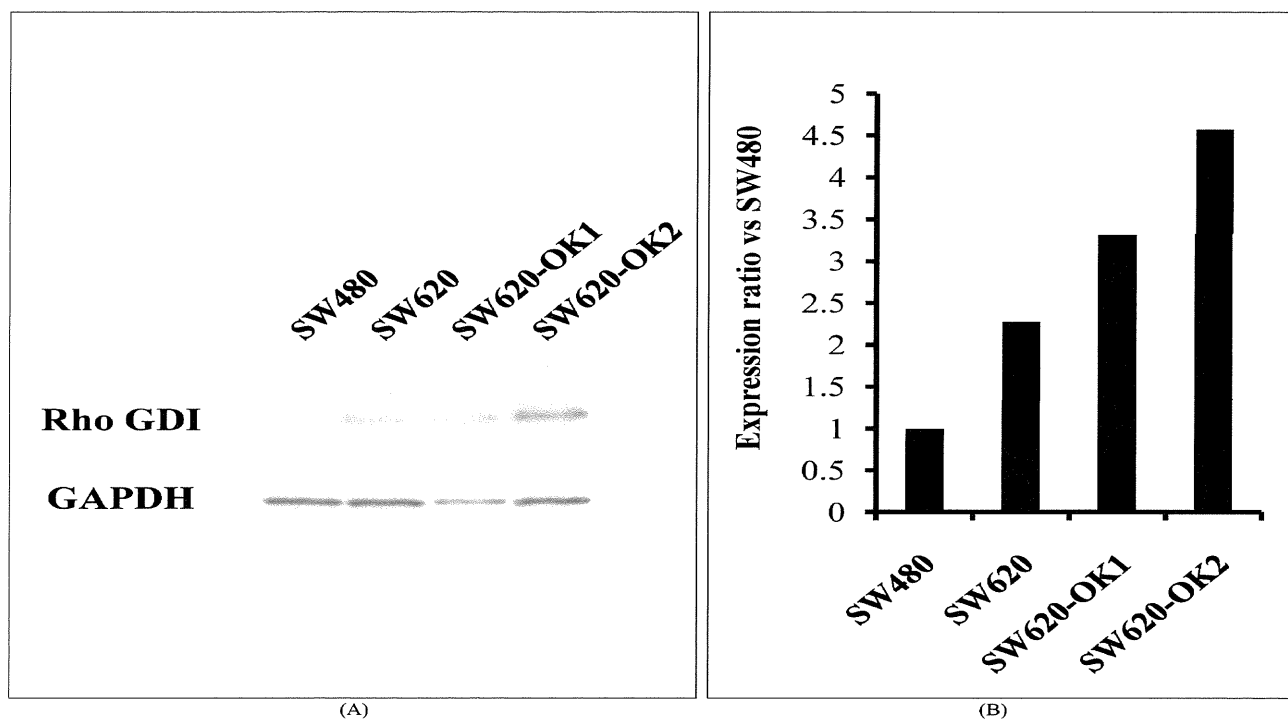


Fig. 2: Rho GDI expression levels in colon cancer cell lines with different metastatic abilities. Rho GDI expression levels in colon cancer cell lines (SW480, SW620, SW620-OK1, SW620-OK2) analyzed by western blotting (A). SW620-OK1, SW620-OK2 have been established as high metastatic sub-lines of SW620 using a mouse metastasis model. Intensity of the western blotting images was quantified by densitometry (B)

vided by the Swiss Institute of Bioinformatics). The search query assumed the following: (i) the peptides were monoisotopic (ii) methionine residues may be oxidized (iii) all cysteines are modified with iodoacetamide.

3.5. TMA Immunochemical staining

TMA slides with human colon cancer samples or multiple cancer samples (Biomax) were de-paraffinated in xylene and rehydrated in a graded series of ethanol washes. Heat-induced epitope retrieval was performed while maintaining the Target Retrieval Solution pH 9 (Dako) at the desired temperature according to manufacturer's instructions. After the treatment, endogenous peroxidase was blocked with 0.3% H₂O₂ in Tris-buffer saline (TBS) for 5 min. After washing twice with TBS, TMA slides were incubated with 10% BSA blocking solution for 30 min. The slides were then incubated with the anti-Rho GDI (Santa Cruz Biotechnology) for 60 min. After washing three times with wash buffer (Dako), each series of sections was incubated for 30 min with Envision + Dual Link (Dako). The reaction products were rinsed twice with wash buffer and then developed in liquid 3, 3'-diaminobenzidine (Dako) for 3 min. After the development, sections were counterstained with Mayer's hematoxylin. All procedures were performed using AutoStainer (Dako).

3.6. TMA Immunohistochemistry scoring

The optimized staining conditions for TMAs corresponding to human colon as well as multiple cancers were determined based on the co-existence of both positive and negative cells in the same tissue sample. Signals were considered positive when reaction products were localized in the expected cellular component. The criteria for scoring of stained tissues were as follows: the distribution score was 0 (0%), 1 (1–50%) or 2 (51–100%), indicating the percentage of positive cells among all tumor cells present in one tissue. The intensity of the signal (intensity score) was scored as 0 (no signal), 1 (weak), 2 (moderate) or 3 (marked). The distribution and intensity scores were then summed into a total score (TS) of TS0 (sum = 0), TS1 (sum = 2), TS2 (sum = 3), and TS3 (sum = 4–5). Throughout this study, TS0 or TS1 was regarded as negative, whereas TS2 or TS3 were regarded as positive.

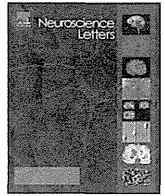
3.7. Western Blot

Expression of Rho GDI in colon cancer cells was detected by anti-Rho GDI (Santa Cruz Biotechnology) and HRP conjugated anti-mouse IgG antibody (Sigma) using the ECL-plus system. Equal amounts of protein loading were confirmed by parallel β -actin immunoblotting, and signal quantification was performed by densitometric scanning.

Acknowledgements: This study was supported in part by Grants-in-Aid for Scientific Research from the Ministry of Education, Culture, Sports, Science and Technology of Japan, and from the Japan Society for the Promotion of Science (JSPS). This study was also supported in part by Health Labor Sciences Research Grants from the Ministry of Health, Labor and Welfare of Japan.

References

- Bishop AL, Hall A (2000) Rho GTPases and their effector proteins. *Biochem J* 348: 241–255.
- Davies RJ, Miller R, Coleman N (2005) Colorectal cancer screening: prospects for molecular stool analysis. *Nat Rev Cancer* 5: 199–209.
- Etienne-Manneville S, Hall A (2002) Rho GTPases in cell biology. *Nature* 420: 629–635.
- Hall A (1997). Rho GTPases and the Actin cytoskeleton. *Science* 279: 509–514.
- Hanash S (2003) Disease proteomics. *Nature* 422: 226–232.
- Imai S, Nagano K, Yoshida Y, Okamura T, Yamashita T, Abe Y, Yoshikawa T, Yoshioka Y, Kamada H, Mukai Y, Nakagawa S, Tsutsumi Y, Tsunoda S (2011). Development of an antibody proteomics system using a phage antibody library for efficient screening of biomarker proteins. *Biomaterials* 32: 162–169.
- Kang S, Kim MJ, An H, Kim BG, Choi YP, Kang KS, Gao MQ, Park H, Na HJ, Kim HK, Yun HR, Kim DS, Cho NH (2010) Proteomic molecular portrait of interface zone in breast cancer. *J Proteome Res* 9: 5638–5645.
- Liu R, Wang K, Yuan K, Wei Y, Huang C (2010) Integrative oncoproteomics strategies for anticancer drug discovery. *Expert Rev Proteomics* 7: 411–429.
- Sahai E (2007). Illuminating the metastatic process. *Nat Rev Cancer* 7: 737–749.
- Suehara Y, Tochigi N, Kubota D, Kikuta K, Nakayama R, Seki K, Yoshida A, Ichikawa H, Hasegawa T, Kaneko K, Chuman H, Beppu Y, Kawai A, Kondo T (2011) Secernin-1 as a novel prognostic biomarker candidate of synovial sarcoma revealed by proteomics. *J Proteomics* 74: 829–842.
- Van Aelst L, D'Souza-Schorey C (1997) Rho GTPases and signaling networks. *Genes Dev* 11: 2295–2322.
- Yoshida Y, Yamashita T, Nagano K, Imai S, Nabeshi H, Yoshikawa T, Yoshioka Y, Abe Y, Kamada H, Tsutsumi Y, Tsunoda S (2011) Limited expression of reticulocalbin-1 in lymphatic endothelial cells in lung tumor but not in normal lung. *Biochem Biophys Res Commun* 405: 610–614.
- Zhao L, Wang H, Li J, Liu Y, Ding Y (2008) Overexpression of Rho GDP-dissociation inhibitor alpha is associated with tumor progression and poor prognosis of colorectal cancer. *J Proteome Res* 7: 3994–4003.



Proteomic analysis of the hippocampus in Alzheimer's disease model mice by using two-dimensional fluorescence difference in gel electrophoresis

Masaoki Takano^a, Takuya Yamashita^{b,c}, Kazuya Nagano^c, Mieko Otani^a, Kouji Maekura^a, Haruhiko Kamada^c, Shin-ichi Tsunoda^c, Yasuo Tsutsumi^{b,c}, Takami Tomiyama^{e,f}, Hiroshi Mori^{e,f}, Kenji Matsuura^d, Shogo Matsuyama^{d,*}

^a Laboratory of Molecular Cellular Biology, School of Pharmaceutical Sciences, Kobe Gakuin University, 1-1-3 Minatojima, Chuo-ku, Kobe 650-8586, Japan

^b Laboratory of Toxicology and Safety Science, Graduate School of Pharmaceutical Sciences, Osaka University, 1-6 Yamadaoka, Suita, Osaka 565-0871, Japan

^c Laboratory of Biopharmaceutical Research, National Institute of Biomedical Innovation, 7-6-8 Saito-Asagi, Ibaraki, Osaka 567-0085, Japan

^d Faculty of Pharmaceutical Sciences, Himeji Dokkyo University, 7-2-1 Kamiohno, Himeji 670-8524, Japan

^e Department of Neuroscience, Osaka City University Graduate School of Medicine, Osaka 545-8585, Japan

^f Core Research for Evolutional Science and Technology, Japan Science and Technology Agency, Japan

HIGHLIGHTS

- ▶ We perform the proteome for APP^{E693Δ}-transgenic mice. Methods are two-dimensional fluorescence difference in gel electrophoresis and mass spectrometry techniques. The expression of 14 proteins are changed in the brain. Aβ oligomers contribute to the expression of proteins.

ARTICLE INFO

Article history:

Received 4 August 2012

Received in revised form 13 October 2012

Accepted 6 November 2012

Keywords:

Proteome

Amyloid β oligomers

Alzheimer's disease

Hippocampus

2D-DIGE

ABSTRACT

We previously identified the E693Δ mutation in amyloid precursor protein (APP) in patients with Alzheimer's disease (AD) and then generated APP-transgenic mice expressing this mutation. As these mice possessed abundant Aβ oligomers from 8 months of age but no amyloid plaques even at 24 months of age, they are a good model to study pathological effects of amyloid β (Aβ) oligomers. The two-dimensional fluorescence difference in gel electrophoresis (2D-DIGE) technology, using a mixed-sample internal standard, is now recognized as an accurate method to determine and quantify proteins. In this study, we examined the proteins for which levels were altered in the hippocampus of 12-month-old APP^{E693Δ}-transgenic mice using 2D-DIGE and liquid chromatography–tandem mass spectrometry (LC–MS/MS). Fourteen proteins were significantly changed in the hippocampus of APP^{E693Δ}-transgenic mice. Actin cytoplasmic 1 (β-actin), heat shock cognate 71 kDa, γ-enolase, ATP synthase subunit β, tubulin β-2A chain, clathrin light chain B (clathrin) and dynamin-1 were increased. Heat shock-related 70 kDa protein 2, neurofilament light polypeptide (NFL), stress-induced-phosphoprotein 2, 60 kDa heat shock protein (HSP60), α-internexin, protein kinase C and casein kinase substrate in neurons protein 1 (Pacsin 1), α-enolase and β-actin were decreased. Western blotting also validated the changed levels of HSP60, NFL, clathrin and Pacsin 1 in APP^{E693Δ}-transgenic mice. The identified proteins could be classified as cytoskeleton, chaperons, neurotransmission, energy supply and signal transduction. Thus, proteomics by 2D-DIGE and LC–MS/MS has provided knowledge of the levels of proteins in the early stages of AD brain.

© 2012 Elsevier Ireland Ltd. All rights reserved.

1. Introduction

AD is neuropathologically characterized by abnormal accumulation of extracellular amyloid plaques and intracellular neurofibrillary tangles throughout cortical and limbic regions. Although the current amyloid cascade hypothesis [6] and tau

hypothesis [15] provide frameworks for studying AD pathogenesis. Recently, diverse lines of evidence suggest that Aβ peptides play more important roles in AD pathogenesis [13,16,20]. Especially, soluble oligomers of Aβ could be a cause of synaptic and cognitive dysfunction in the early stages of AD. To address the relationship between Aβ oligomers and pathological features of AD, we generated APP transgenic mice expressing the E693Δ mutation, which enhanced Aβ oligomerization without fibrillization [25]. It might provide a clue for elucidating AD pathology caused by Aβ oligomers to analyze the APP^{E693Δ}-transgenic mice.

* Corresponding author. Tel.: +81 79 223 6849; fax: +81 79 223 6857.

E-mail address: shogo@himeji-du.ac.jp (S. Matsuyama).

One of the most utilized approaches in proteomics to quantify and identify proteins is two dimensional gel electrophoresis (2DE) and mass spectrometry (MS) [5]. Proteomic approaches were most widely based on methods using differential expression on 2D-PAGE gels, or more recently 2D chromatography, followed by mass spectrometry protein identification. Compared to these conventional analyses, 2D-DIGE has higher reproducibility and sensitivity because of its internal standard design which minimizes gel-to-gel variation, improves spot matching, reduces number of gels needed, and permits quantitative analysis of small sample amounts.

In this study, we studied the altered expression of proteins in the hippocampus of APP_{E693Δ}-transgenic mice using 2D-DIGE and LC-MS/MS approach. This approach revealed that the levels of at least 14 proteins were altered in the hippocampus of 12-month-old APP_{E693Δ}-transgenic mice. These findings suggest that Aβ oligomers might cause synaptic and cognitive dysfunction by affecting the expression of these proteins in the hippocampus.

2. Experimental procedures

2.1. Materials

Sodium dodecyl sulfate, urea, thiourea, CHAPS, dithiothreitol, iodoacetamide, bromophenol blue, and RNase A and DNase I for SDS-PAGE or 2DE were all obtained from Wako Pure Chemical Industries (Osaka, Japan). Source information for all other assay reagents and materials are incorporated into their respective assay methods described below.

2.2. Animal subjects

Transgenic mice expressing human APP₆₉₅ with the APP_{E693Δ} mutation under the mouse prion promoter were used [25]. Heterozygous human APP_{E693Δ}-transgenic mice and age-matched non-transgenic littermates were sacrificed at 12 months of age, and their hippocampi were isolated on an ice-cold plate. Animal care and handling were performed strictly in accordance with the Guidelines for Animal Experimentation at Kobe Gakuin University and Himeji Dokkyo University. Every effort was made to minimize the number of animals used and their suffering.

2.3. Protein labeling with CyDyes

Equal amounts of total protein from 4 hippocampi of APP_{E693Δ}-transgenic mice or age-matched non-transgenic littermates were separately pooled. Protein samples were labeled with CyDyes (GE Healthcare, Piscataway, NJ), as per manufacturer's instructions. In brief, 50 μg of total protein from each sample was mixed in a tube and labeled with Cy2 minimal dye, and 50 μg protein taken from the mix was used as an internal standard on each gel for the three subsequent 2DE and image analysis. In parallel, 50 μg protein from each sample was labeled with either Cy3 or Cy5, and the dyes scrambled within each group to avoid possible dye bias. As a result, one replicate was Cy3 labeled proteins and another replicate was Cy5 labeled proteins. Two replicates (Cy3 and Cy5 labeled samples) were mixed, divided and applied each three independent gels. The sample volumes were adjusted to 18 μL with labeling buffer (7M urea, 2 M thiourea, 4% CHAPS, 30 mM Tris), followed by addition of 1 μL dye (working solution) to each individual sample. The samples were left on ice for 30 min in the dark, followed by adding 1 μL of 10 mmol/L lysine to stop the reaction.

2.4. 2D electrophoresis and image analysis

One sample from each of the CyDye groups was mixed together and adjusted to final concentrations of 1% DTT, 1% IPG buffer

at a total volume of 350 μL with lysis buffer (7M urea, 2M thiourea, 4% CHAPS) and was used to 24 cm pH 4–7 IPG strips (non-linear; GE Healthcare, Piscataway, NJ) overnight. First dimension isoelectric focusing (IEF) was carried out with IPGphor II (GE Healthcare, Piscataway, NJ). Second dimension SDS-PAGE was performed by mounting the IPG strips onto 20 × 26 cm 12.5% DIGE gels (GE Healthcare, Piscataway, NJ) using Ettan DALT six Large Electrophoresis System (GE Healthcare, Piscataway, NJ) and running the gels at 16 mA/gel for the initial hour and 25 mA/gel at 25 °C constantly until bromophenol blue reached the bottom of the gel. The lysates were labeled at the ratio of 50 μg proteins: 400 pmol Cy3 or Cy5 protein-labeling dye (GE Healthcare Biosciences) in dimethylformamide according to the manufacturer's protocol.

In summary, three analytical gels were completed in total, running 25 μg of pooled reference sample labeled with Cy2, along with two samples (25 μg each), one labeled with Cy3 and the other labeled with Cy5. Gels selected for picking were stained with Deep purple (GE Healthcare, Piscataway, NJ). Approximately 1100 spots were matched across all three analytical gels. The analytical gel was picked using an automated robotic system, Ettan Spot picker (GE Healthcare, Piscataway, NJ). The pick list was created based on the Deep purple image. 2 mm gel plugs were picked, washed, reduced and alkylated, and then digested with trypsin, and the resulting peptides were extracted. Gel trypsinization was performed as previously described [24].

2.5. LC/MS/MS identification

Trypsinized peptides were analyzed by nano LC/MS/MS on a ThermoFisher LTQ Orbitrap XL. In brief, 30 mL of hydrolysate was loaded onto a 5 mm 675 mm ID C12 (Jupiter Proteo, Phenomenex) vented column at a flow-rate of 10 mL/min. Gradient elution was conducted on a 15 cm by 75 mm ID C12 column at 300 nL/min. A 30 min gradient was employed. The mass spectrometer was operated in a data-dependent mode, and the six most abundant ions were selected for MS/MS. Mass spectrometry results were searched using Mascot (www.matrixscience.com). Samples were processed in the Scaffold algorithm using DAT files generated by Mascot. Parameters for LTQ Orbitrap XL data require a minimum of two peptide matches per protein with minimum probabilities of 90% at the protein level.

2.6. Western blotting

Approximately 25 μg of protein from mouse hippocampus was applied to a 12.5% acrylamide gel and SDS-polyacrylamide gel electrophoresis was performed at 17.5 mA/gel for 2 h in second dimension. The gels were transferred onto PVDF membranes (Pall Corporation, Pensacola, FL, USA), in a trans-blot electrophoresis transfer cell (Nihon Eido, Tokyo, Japan). Western blotting was performed by using monoclonal antibodies against β-actin (diluted 1:1000, Cell Signaling, USA) and clathrin (diluted 1:250, Abcam, USA), polyclonal antibodies HSP60, NFL, voltage-dependent anion-selective channel protein 1 (VDAC) (diluted 1:1000, Cell Signaling, USA) and Paccin 1 (diluted 1:500, Millipore, USA). Peroxidase-conjugated antibody (diluted 1:5000, Abcam, USA) was used as secondary antibody. The reaction was detected by chemiluminescence with ECL reagents (Pierce Biotechnology, USA). A semi quantitative analysis based on optical density was performed by ImageJ software (available at <http://www.rsweb.nih.gov/ij>).

3. Results and discussion

The 2D-DIGE gels of the hippocampi from wild type and APP_{E693Δ}-transgenic mice pools were shown as Fig. 1. Two replicates of each pooled sample were run, labeling one replicate with

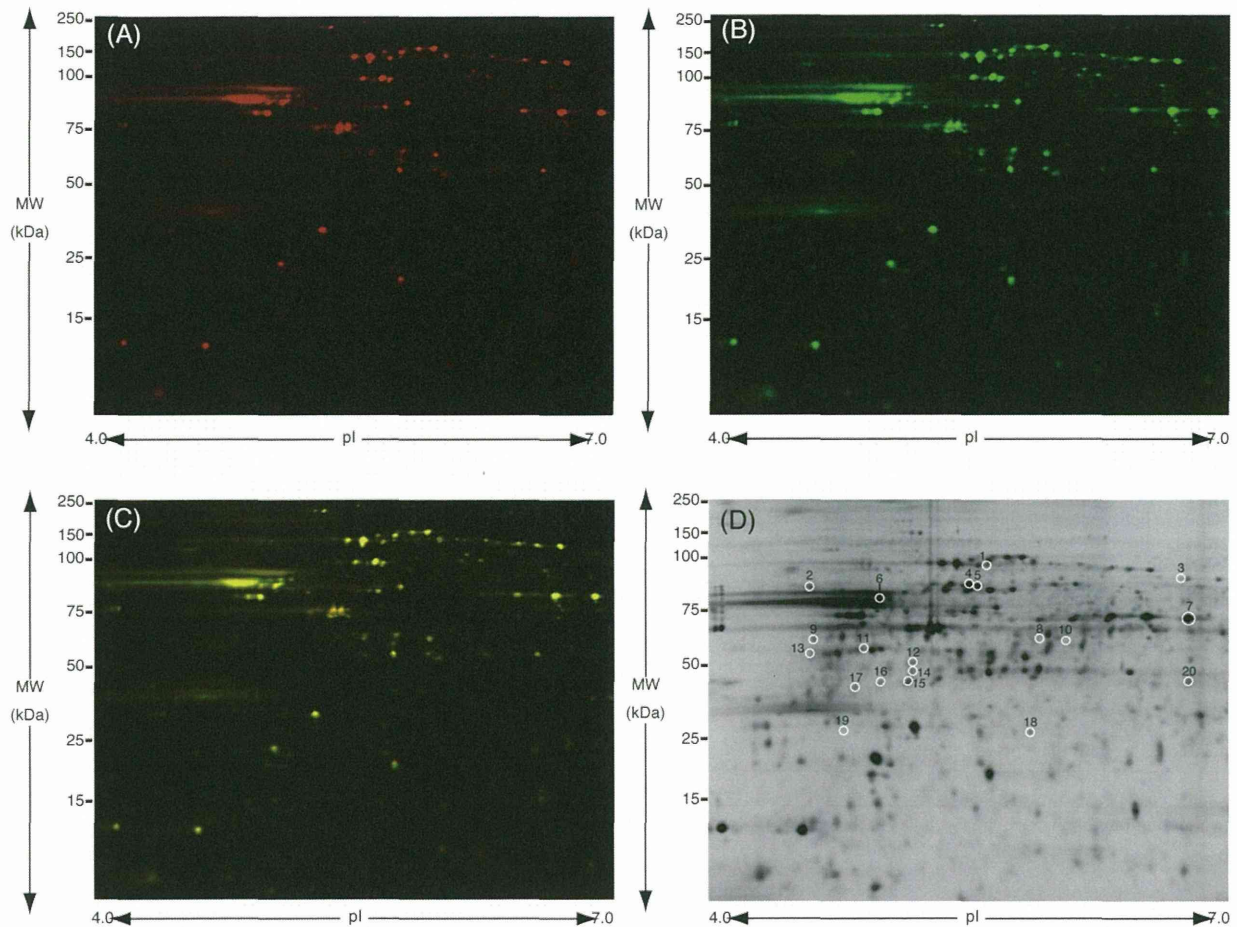


Fig. 1. 2D-DIGE gel image of fluorescence-labeled hippocampal proteins of non-transgenic and APP_{E693Δ}-transgenic mice. (A) Analysis of the proteome of non-transgenic mice hippocampi with Cy3 Dye. (B) APP_{E693Δ}-transgenic mice hippocampi with Cy5 Dye. (C) Merged. (D) Fourteen protein spots identified from non-transgenic and APP_{E693Δ}-transgenic mice hippocampi by LC/MS/MS. Black numbers with white circles indicate proteins that are listed in Table 1.

Cy3 (Fig. 1A) and one replicate with Cy5 (Fig. 1B), resulting in three analytical gels. The 2D-DIGE comparative analysis of the wild type and APP_{E693Δ}-transgenic mice revealed significant 74 spots (Fig. 1C). These spots were investigated by LC-MS/MS (Fig. 1D). Finally, fourteen proteins were identified as shown in Table 1. These proteins are classified into several groups that are involved in cytoskeletal, chaperone, energy metabolic, vesicle transport and signaling proteins (Table 2).

Spot nos. 1, 3 and 4 were identified as heat shock-related 70 kDa protein 2, stress-induced-phosphoprotein 1 and HSP60, respectively. The stress-induced-phosphoprotein 1 is the co-chaperone and thought of the function in regulation of interaction with Hsp70 and Hsp90 [10]. HSP60 is the chaperon which is implicated in mitochondrial protein import and macromolecular assembly and may facilitate the correct folding of imported proteins [9]. The amounts of heat shock-related 70 kDa protein 2, stress-induced-phosphoprotein 1, and HSP60 were significantly decreased. On the contrary, spot no. 9 which was identified as heat shock cognate 71 kDa protein was significantly increased. This protein is also the chaperone and acts as a repressor of transcriptional activation [8]. Thus, Aβ oligomers might contribute to changing the expression of the chaperons.

Spot nos. 8, 10–12 and 16 were identified as actin, and spot nos. 15 and 17 were identified as tubulin β-2A chain. Actin is one of the major cytoskeletal proteins in neurons, and the dynamics of its assembly are involved in many aspects of cell motility, vesicle transport, and membrane turnover [14]. Actin itself is known to link with Aβ, which enhances the neurotoxicity induced by

tau-mediated actin filament formation [4]. The four spots of actin but not no. 12 and those of tubulin were significantly increased. Thus, Aβ oligomers might lead to increasing the amounts of actin and tubulin.

Spot nos. 5 and 2 were identified as α-interneixin and NFL, respectively, which are known as neuronal intermediate proteins [2,18]. The amounts of α-interneixin and NFL were significantly decreased. Thus, the decreased amounts of NFL and interneixin might raise neural dysfunction in the hippocampus of AD.

Spot nos. 7 and 13 were identified as α-enolase. Spot nos. 14 and 19 were identified as γ-enolase and ATP synthase subunit β, respectively. Enolase is a multifunctional protein as glycolytic enzyme, belonging to a novel class of surface proteins [11]. ATP synthase is a key role enzyme that provides energy for the cell to use through the synthesis of ATP [1]. The amount of α-enolase was significantly decreased, but the amounts of γ-enolase and ATP synthase subunit β were significantly increased. Interestingly, the levels of α-enolase and ATP synthase subunit α mitochondrial proteins significantly increased in the hippocampus of J20Tg mice with amyloid deposition [19]. The amyloid deposit enhanced the expression of energy metabolic proteins [22]. Combined with our findings, both Aβ oligomers and amyloid deposition might play an important role in the change of energy metabolic proteins as α-enolase, γ-enolase and ATP synthase subunit β.

Spot no. 20 was identified as dynamin. Dynamin, a well studied neuron-specific mechanochemical GTPase, pinches off synaptic vesicles, freeing them from the membrane and allowing them to re-enter the synaptic vesicle pool to be refilled for future release

Table 1
Identified proteins from differentially expressed in the hippocampus of APP_{E693Δ}-transgenic mice when compared to non-transgenic littermates.

Spot no.	Protein ID	Fold (APP/WT)	t-Test	Accession	Coverage	#Peptides	Predicted MW (kDa)	Calc. pI	Score
1	Heat shock-related 70 kDa protein 2	-1.32	0.040	P14659	26.22	23	69.6	5.67	625.70
2	Neurofilament light polypeptide	-1.48	0.002	P08551	39.96	43	61.5	4.64	1004.84
3	Stress-induced-phosphoprotein 1	-1.44	0.002	Q60864	16.21	9	62.5	6.80	157.49
4	60 kDa heat shock protein	-1.36	0.013	P63038	52.71	71	60.9	6.18	1916.39
5	Alpha-internexin	-1.34	0.023	P46660	42.66	39	55.7	5.27	1119.47
6	Protein kinase C and casein kinase substrate in neurons protein 1	-1.48	0.023	Q61644	28.34	15	50.5	5.24	356.92
7	Alpha-enolase	-1.32	0.000	P17182	34.33	24	47.1	6.80	474.21
8	Actin, cytoplasmic 1	1.51	0.003	P60709	25.87	14	41.7	5.48	231.79
9	Heat shock cognate 71 kDa protein	1.35	0.015	P63017	12.54	16	70.8	5.52	319.85
10	Actin, cytoplasmic	1.34	0.004	P60709	24.27	13	41.7	5.48	279.37
11	Actin, cytoplasmic 1	1.38	0.022	P60709	15.47	7	41.7	5.48	243.14
12	Actin, cytoplasmic 1	-1.56	0.013	P60709	22.67	12	41.7	5.48	131.57
13	Gamma-enolase	1.33	0.005	P17183	20.05	13	47.3	5.11	237.25
14	ATP synthase subunit beta	1.40	0.047	P56480	23.60	18	56.3	5.34	356.19
15	Tubulin beta-2A chain	1.31	0.021	Q13885	14.83	13	49.9	4.89	313.07
16	Actin, cytoplasmic 1	1.47	0.002	P60709	6.93	3	41.7	5.48	97.01
17	Tubulin beta-2S chain	1.44	0.009	Q13885	11.46	5	49.9	4.89	118.50
18	Clathrin light chain B	1.68	0.005	P09497	8.30	3	25.2	4.64	95.06
19	ATP synthase subunit beta	1.46	0.013	P06576	16.64	16	56.5	5.40	283.06
20	Dynamin-1	1.40	0.006	Q05193	9.61	13	97.3	7.17	242.16

Mass spectrometry protein identification of 2D-DIGE spots of interest and statistical analysis using *t*-test between wild type mice and APP_{E693Δ}-transgenic mice gels ($P < 0.05$). The proteins of mouse hippocampus were separated by 2DE and identified by LC MS/MS, following in-gel digestion with trypsin. The spots representing identified proteins are indicated in Fig. 1D and are designated with their ID accession numbers of Swiss Prot database. Score relates to the probability assignment. Score and sequence coverage were calculated by MASCOT search engine (<http://www.matrixscience.com>).

Table 2
Functions regulated by proteins that showed an altered expression in APP_{E693Δ}-transgenic mouse hippocampus.

Function	Identified protein	Up/down
Cytoskeletal and their interacting proteins	Neurofilament light polypeptide	Down
	Alpha-internexin	Down
	Actin, cytoplasmic 1	Up/down
	Tubulin β-2A Chain	Up
Chaperone and their interacting proteins	Stress-induced-phosphoprotein 1	Down
	60 kDa heat shock protein	Down
	Heat shock cognate 71 kDa protein	Down
Energy metabolic proteins	Alpha-enolase	Down
	Gamma-enolase	Up
	ATP synthase subunit beta	Up
Vesicle transport and recycling	Dynamin-1	Up
	Clathrin light chain B	Up
Signaling proteins	Protein kinase C and casein kinase substrate in neurons protein 1	Down

The analysis of proteins function was done by using MOTIF (<http://www.genome.jp/tools/motif/>).

[12]. The amount of dynamin was significantly increased. Our findings in APP_{E693Δ}-transgenic mice without plaque deposition are consistent with previous findings that protein levels of dynamin were increased in Tg2576 mice with plaque deposition [21], suggesting that the release of neurotransmitter is affected by dynamin

increased irrespective of AD stage. Also, spot no. 6 was identified as Pascin 1. The Pascin 1 is colocalized, oligomerized and bound with dynamin, and both proteins participate in synaptic vesicle endocytosis [17]. The amount of Pascin 1 was significantly increased. Taken together, Pascin 1 and dynamin enhanced by Aβ oligomers

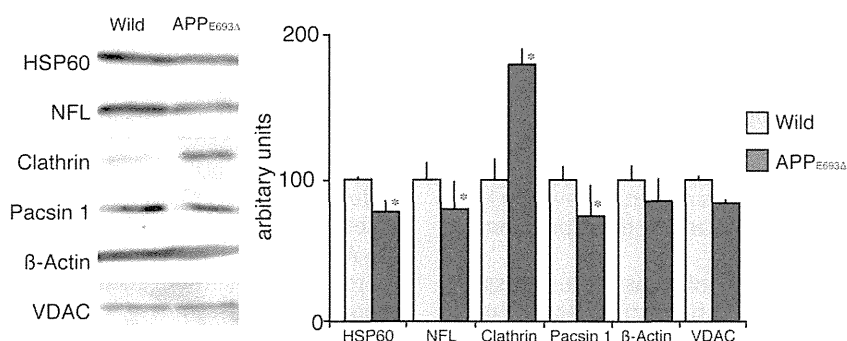


Fig. 2. Differentially expressed proteins validated by Western blotting for the hippocampus of non-transgenic and APP_{E693Δ}-transgenic mice. (A) The levels of HSP60, NFL, clathrin, Pascin 1, β-actin and VDAC in individual samples of each group were detected. (B) Graphical representation of the semi quantitative analysis (mean ± SEM of O.D. of bands). Data are presented as mean ± SEM ($n = 4$) *t*-test; * $P < 0.05$ vs. APP_{E693Δ}-transgenic mice.

might change the function of synaptic vesicle in the hippocampus of AD.

Spot no. 18 was identified as clathrin, which is known as the major protein of the polyhedral coat of coated pits and vesicles [7]. The amount of spot no. 18 was significantly decreased. APP was associated clusters of clathrin-coated vesicles and endosomes [3]. Thus, A β oligomers might inhibit the vesicle formation by clathrin.

In addition, we performed a validation experiment for HSP60, NFL, clathrin, Pacsin 1 and β -actin as the altered proteins, and VDAC as the unchanged protein (as control) [23]. The increased levels of clathrin, the decreased levels of HSP60, NFL, and Pacsin 1 and the unchanged level of β -actin and VDAC in APP_{E693 Δ} -transgenic mice hippocampus were validated by Western blotting (Fig. 2).

In summary, we identified the altered levels of 14 proteins in APP_{E693 Δ} -transgenic mice hippocampus using 2D-DIGE and LC-MS/MS approach. This approach elucidated the pathological effects of A β oligomers on hippocampus. Our findings might provide a clue for investigation of the hippocampus of AD early stage.

Acknowledgements

This work was supported by grants from Kobe Gakuin University for Collaborative Research C and the Smoking Research Foundation. The authors thank Dr. Tadanori Mayumi for his encouragement during the early days of the study.

References

- [1] U. Andersson, H. Antonicka, J. Houstek, B. Cannon, A novel principle for conferring selectivity to poly(A)-binding proteins: interdependence of two ATP synthase beta-subunit mRNA-binding proteins, *Biochemical Journal* 346 (Pt 1) (2000) 33–39.
- [2] C.L. Chien, R.K. Liem, Characterization of the mouse gene encoding the neuronal intermediate filament protein alpha-internexin, *Gene* 149 (1994) 289–292.
- [3] A. Ferreira, A. Caceres, K.S. Kosik, Intraneuronal compartments of the amyloid precursor protein, *Journal of Neuroscience* 13 (1993) 3112–3123.
- [4] T.A. Fulga, I. Elson-Schwab, V. Khurana, M.L. Steinhilb, T.L. Spiers, B.T. Hyman, M.B. Feany, Abnormal bundling and accumulation of F-actin mediates tau-induced neuronal degeneration in vivo, *Nature Cell Biology* 9 (2007) 139–148.
- [5] A. Gorg, C. Obermaier, G. Boguth, A. Harder, B. Scheibe, R. Wildgruber, W. Weiss, The current state of two-dimensional electrophoresis with immobilized pH gradients, *Electrophoresis* 21 (2000) 1037–1053.
- [6] J. Hardy, D.J. Selkoe, The amyloid hypothesis of Alzheimer's disease: progress and problems on the road to therapeutics, *Science* 297 (2002) 353–356.
- [7] J. Hirst, M.S. Robinson, Clathrin and adaptors, *Biochimica et Biophysica Acta* 1404 (1998) 173–193.
- [8] C.R. Hunt, A.J. Parsian, P.C. Goswami, C.A. Kozak, Characterization and expression of the mouse Hsc70 gene, *Biochimica et Biophysica Acta* 1444 (1999) 315–325.
- [9] S. Ikawa, R.A. Weinberg, An interaction between p21ras and heat shock protein hsp60, a chaperonin, *Proceedings of the National Academy of Sciences* 89 (1992) 2012–2016.
- [10] J.L. Johnson, A. Halas, G. Flom, Nucleotide-dependent interaction of *Saccharomyces cerevisiae* Hsp90 with the cochaperone proteins Sti1, Cpr6, and Sba1, *Molecular and Cellular Biology* 27 (2007) 768–776.
- [11] M. Kaghad, X. Dumont, P. Chalou, J.M. Lelias, N. Lamande, M. Lucas, M. Lazar, D. Caput, Nucleotide sequences of cDNAs alpha and gamma enolase mRNAs from mouse brain, *Nucleic Acids Research* 18 (1990) 3638.
- [12] B.L. Kelly, R. Vassar, A. Ferreira, Beta-amyloid-induced dynamin 1 depletion in hippocampal neurons. A potential mechanism for early cognitive decline in Alzheimer disease, *Journal of Biological Chemistry* 280 (2005) 31746–31753.
- [13] W.L. Klein, G.A. Krafft, C.E. Finch, Targeting small Abeta oligomers: the solution to an Alzheimer's disease conundrum? *Trends in Neurosciences* 24 (2001) 219–224.
- [14] T.B. Kuhn, P.J. Meberg, M.D. Brown, B.W. Bernstein, L.S. Minamide, J.R. Jensen, K. Okada, E.A. Soda, J.R. Bamberg, Regulating actin dynamics in neuronal growth cones by ADF/cofilin and rho family GTPases, *Journal of Neurobiology* 44 (2000) 126–144.
- [15] V.M. Lee, M. Goedert, J.Q. Trojanowski, Neurodegenerative tauopathies, *Annual Review of Neuroscience* 24 (2001) 1121–1159.
- [16] S. Li, S. Hong, N.E. Shepardson, D.M. Walsh, G.M. Shankar, D. Selkoe, Soluble oligomers of amyloid Beta protein facilitate hippocampal long-term depression by disrupting neuronal glutamate uptake, *Neuron* 62 (2009) 788–801.
- [17] J. Modregger, B. Ritter, B. Witter, M. Paulsson, M. Plomann, All three PACSIN isoforms bind to endocytic proteins and inhibit endocytosis, *Journal of Cell Science* 113 (Pt 24) (2000) 4511–4521.
- [18] R.A. Nixon, R.K. Sihag, Neurofilament phosphorylation: a new look at regulation and function, *Trends in Neurosciences* 14 (1991) 501–506.
- [19] R.A. Robinson, M.B. Lange, R. Sultana, V. Galvan, J. Fombonne, O. Gorostiza, J. Zhang, G. Warriar, J. Cai, W.M. Pierce, D.E. Bredesen, D.A. Butterfield, Differential expression and redox proteomics analyses of an Alzheimer disease transgenic mouse model: effects of the amyloid-beta peptide of amyloid precursor protein, *Neuroscience* 177 (2011) 207–222.
- [20] D.J. Selkoe, Alzheimer's disease is a synaptic failure, *Science* 298 (2002) 789–791.
- [21] S.J. Shin, S.E. Lee, J.H. Boo, M. Kim, Y.D. Yoon, S.I. Kim, I. Mook-Jung, Profiling proteins related to amyloid deposited brain of Tg2576 mice, *Proteomics* 4 (2004) 3359–3368.
- [22] R. Sultana, D. Boyd-Kimball, J. Cai, W.M. Pierce, J.B. Klein, M. Merchant, D.A. Butterfield, Proteomics analysis of the Alzheimer's disease hippocampal proteome, *Journal of Alzheimer's Disease* 11 (2007) 153–164.
- [23] M. Takano, K. Maekura, M. Otani, K. Sano, T. Nakamura-Hirota, S. Tokuyama, K.S. Min, T. Tomiyama, H. Mori, S. Matsuyama, Proteomic analysis of the brain tissues from a transgenic mouse model of amyloid beta oligomers, *Neurochemistry International* 61 (2012) 347–355.
- [24] M. Takano, M. Otani, A. Sakai, K. Kadoyama, S. Matsuyama, A. Matsumoto, M. Takenokuchi, M. Sumida, T. Taniguchi, Use of a phosphosensor dye in proteomic analysis of human mutant tau transgenic mice, *Neuroreport* 20 (2009) 1648–1653.
- [25] T. Tomiyama, S. Matsuyama, H. Iso, T. Umeda, H. Takuma, K. Ohnishi, K. Ishibashi, R. Teraoka, N. Sakama, T. Yamashita, K. Nishitsuji, K. Ito, H. Shimada, M.P. Lambert, W.L. Klein, H. Mori, A mouse model of amyloid beta oligomers: their contribution to synaptic alteration, abnormal tau phosphorylation, glial activation, and neuronal loss in vivo, *Journal of Neuroscience* 30 (2010) 4845–4856.

